2019 American Control Conference (ACC)
Philadelphia, PA, USA, July 10-12, 2019

A stepped-sine curve-fit algorithm for finding cantilever resonance shifts in AFM

Zhixin Kang[1], Verda Saygin[1], Keith A. Brown[1,2,3] and Sean Andersson [1,4]
[1]Department of Mechanical Engineering, [2]Division of Materials Science and Engineering,
[3]Department of Physics, and [4]Division of Systems Engineering
Boston University, Boston, MA 02215
{sheliak,saygin,brownka,sanderss}@bu.edu

***Abstract*— Atomic force microscopes (AFMs) are used not only to image with nanometer-scale resolution, but also to nanofabricate structures on a surface using methods such as dip-pen nanolithography (DPN). DPN involves using the tip of the AFM to deposit a small amount of material on the surface. Typically, this process is done in open loop, leading to large variations in the amount of material transferred. One of the first steps to closing this loop is to be able to accurately and rapidly measure the amount of deposition. This can be done by measuring the change in the resonance frequency of the cantilever before and after a write as that shift is directly related to the change in mass on the cantilever. Currently, this is done using a thermal-based system identification, a technique which uses the natural Brownian excitation of the cantilever as a white noise excitation combined with a fast Fourier transform to extract a Bode plot. However, thermal-based techniques do not have a good signal to noise ratio at typical cantilever resonance frequencies and thus do not provide the needed resolution in the DPN application. Here we develop a scheme that iteratively uses a stepped-sine approach. At each step of the iteration, three frequencies close to the approximate location of the resonance are injected and used to fit a model of the magnitude of the transfer function. The identified peak is used to select three new frequencies in a smaller range in a binary search to reduce the uncertainty of the measured resonance peak location. The scheme is demonstrated through simulation and shown to produce an accuracy of better than 0.5 Hz on a cantilever with a 14 kHz resonance in a physically realistic noise scenario.**

I. Introduction

The atomic force microscope (AFM) is a powerful imaging tool for studying with nanometer precision a wide range of surface properties, including topography, material moduli, and surface potential [1]–[4]. It is also being increasingly used to study dynamics at the nanometer scale [5]–[7]. In general, the relative vertical position of a sharp probe and the surface is regulated by using feedback to control either the deflection of the cantilever (in contact mode) or the amplitude of oscillation (in intermittent contact, also known as tapping, mode) [8]–[11]. The desired information is then extracted from the control signal.

In this paper, we consider the use of AFM in a non-imaging domain, in particular in Dip-Pen Nanolithography (DPN). DPN is a method for nanofabrication in which the AFM probe is coated with small molecules, a liquid, or a gel [12]–[14] and then used to deposit that material repeatedly on a substrate of interest. This local transfer method of patterning has attracted significant interest because of its ability to write materials additively with sub-100 nm resolution [15], [16]. DPN has been successfully used to pattern with a variety of substrates and inks. It is currently the highest resolution method for doing additive manufacturing using soft materials and can be applied in application domains ranging from nano-electronics to medical diagnostics [17].

It is of interest to pattern features accurately and precisely, both in terms of their physical location and the amount of material deposited. While the high spatial resolution is naturally provided by the AFM, the ability to write features of well-controlled sizes is an ongoing challenge. The amount of material which is deposited on the surface is a function of many physical effects that depend on, among other things, the surface forces. As a result, the formation and rupture of liquid bridges exhibits large variation depending on the size (molecular weight) of the inks, the amount of ink on the probe, and the environmental conditions, leading to vastly different experimental results under the same write parameters [17]. The overarching goal of this work, illustrated in Fig. 1, is to enhance the repeatability and controllability of DPN by using feedback control to adjust the patterning process to ensure the patterns produced are consistent in size as well as spatial location.

Fig. 1: Illustration of a controlled patterning process leading to equally space, equally sized features written to the surface.

In this paper, we present a scheme that combines stepped-sine measurements with a binary search. Stepped-sine is a non-parametric demodulation that involves stimulating the system with a signal and measuring the response [18]. The response at each individual frequency can be measured both quickly and precisely. Because of the nanometer-scale of the setup, we assume that surface tension is dominant and thus that no mass is lost during the sinusoidal excitation of the

978-1-5386-7926-5/$31.00 ©2019 AACC

cantilever. For full system identification, the need to sweep the driving sinusoid over a wide range of frequencies leads to long measurement times. In our setting, though, we have prior information on the approximate location of the peak and no need to identify the dynamics over the entire frequency spectrum. As a result, we can focus signals in a narrow band as we hone in on the resonance.

The remainder of this paper is organized as follows. We first introduce the techniques involved in a patterning process in Sec. II, then briefly describe the use of a thermal measurement for system identification of cantilever dynamics in AFM, giving experimental results to demonstrate the typical resolution achieved in Sec. III. In Sec. IV we describe the use of stepped- (also known as swept-) sine before presenting the overall algorithm in Sec. V. The scheme in physically realistic simulations follows in Sec. VI, in which we compare our method to a standard thermal-based measurement. We end with a few concluding remarks in Sec. VII.

II. Patterning Process

To write a feature in DPN, the probe is first coated by dipping it in a reservoir of interest and then moved to a desired location. A force-distance (F-D) curve is then performed (Fig. 2). In order to develop a closed-loop controller, it is necessary to have a measurement of the amount of ink deposited. A natural way to do this is to measure the change in the resonance frequency of the cantilever before and after the write since that frequency is directly related to the mass of the cantilever. Micro-cantilevers are capable of

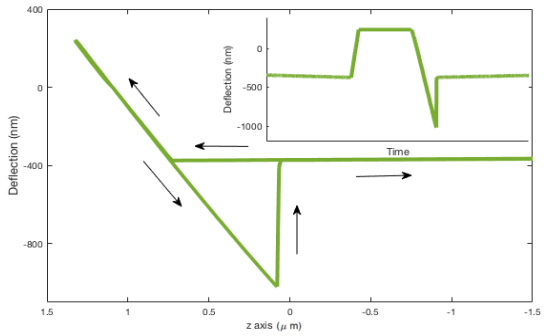

Fig. 2: Illustration of a force-distance curve. The deflection of the cantilever is represented as a function of the displacement of the piezo-actuator in the z-axis. (The inset graph indicates the deflection as a function of time.) As the tip approaches the surface (arrows pointing left), deflection increases until a set force is reached. After a dwell time, the actuator retracts (arrows pointing right). Adhesion between the tip and the sample leads to a different retraction path since a larger force is needed to pull the tip off the surface.

highly sensitive detection of changes in mass adhering to the cantilever through changes in cantilever resonant frequency [19]. Mass detection is achieved by using the mass-spring equation given by

$$f_{res} = \frac{1}{2\pi}\sqrt{\frac{k}{m_{eff} + \delta m}}, \tag{1}$$

where f_{res} is the measured resonant frequency, k is the spring constant, m_{eff} is the mass of the cantilever, and δm is the mass of the liquid attached to the tip of the cantilever. In practice, the magnitude of the frequency shift depends on the mechanical properties of the cantilever and the amount of ink deposited. For a typical contact mode cantilever with a 0.3 N/m spring constant and a 14 kHz resonance frequency, the needed resolution to measure the frequency shift when writing a 2 μm diameter feature on a hydrophobic surface is on the order of 1 Hz.

During patterning in DPN, the resonance of the cantilever shifts to a higher frequency after each write due to the decrease of mass of ink on the probe. This is illustrated in the experimental curves in Fig. 3. The figure shows the Lorentzian curve fits to measured data at the beginning of the process and after each of four successive writes. Details on the identification process (known as a thermal) are given in Sec. III. In this experiment, very large features were written, leading to shifts of between 20-40 Hz. In practice, much smaller features with frequency shifts on the order of 1 Hz are desired.

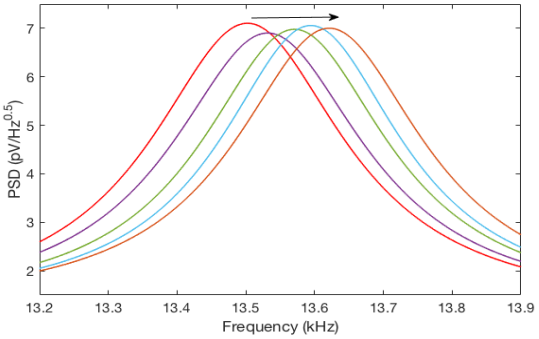

Fig. 3: Experimental results of the resonant frequency shift after successive writes in a DPN patterning process. As the mass is deposited for each write, the peak frequency shifts to the right since the mass remaining on the probe decreases.

III. Thermal Measurement

The standard method used on many commercial AFMs to identify the cantilever dynamics is generally referred to as a *thermal*. A thermal uses the free random motion of the cantilever as a white noise input and measures the resulting motion of the cantilever. This measurement is analyzed using a Fast Fourier Transform (FFT) to generate a Power Spectral Density (PSD). Each peak in the PSD can be fit to a modified Lorentzian, given by

$$L(x) = c + a\frac{\beta^2}{\beta^2 + (x - x_0)^2}, \tag{2}$$

where c is the PSD offset, a is the frequency offset, β is half of the peak width, x_0 is the peak frequency and x is the measured frequency. The approach does not require any external drive signal and is a relatively fast way to do system identification as all frequencies are excited and measured at the same time. Researchers have used this thermal method

to detect mass on the cantilever but only with frequencies on the order of 100 to 1,000 Hz [19].

A typical example of a thermal is shown in Fig 4 where data was acquired using a commercial AFM (MFP-3D, Asylum Research) outfitted with a typical contact mode cantilever (PPP-CONT, Nanosensor). As shown in the figure, this method identifies not only the first resonance but also the higher order harmonics.

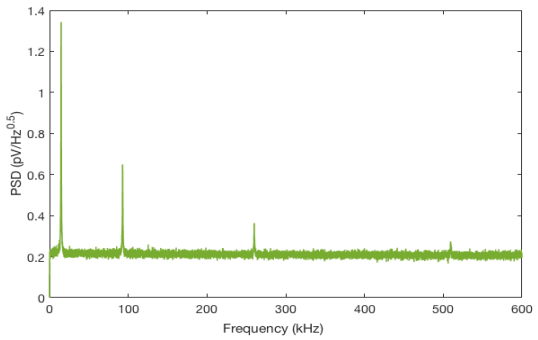

Fig. 4: Experimental PSD acquired using a thermal tune on an Asylum Research MFP-3D. The first resonance is at 13.5 kHz. Higher order harmonics are also clearly evident.

As noted above, identification of the resonant frequency is done by fitting the PSD with a Lortezian. A fit to the first peak in the experimental thermal of Fig. 4 is shown in Fig. 5.

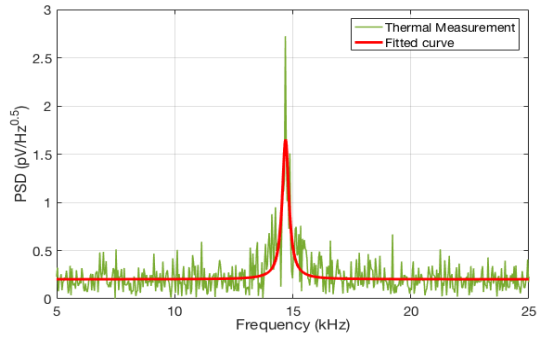

Fig. 5: A Lorentzian fit to the first peak of a thermal.

Due to the poor signal-to-noise ratio (SNR) of a thermal, particularly at the high frequencies typical to cantilever resonances, the achievable resolution is typically much worse than the desired 1 Hz. To increase the SNR, data can be averaged over many repeated measurements. In general, the higher the resonance frequency to be identified, the more iterations are needed. We explored the effect of averaging curves to improve the SNR through experiment, using up to 300 averaged measurements (recall that a *measurement* here is an entire thermal). Experiments were repeated ten times to obtain the standard deviation of the resonance frequency.

The results, shown in Fig. 6, indicate that the uncertainty quickly decreases as the number of measurements in the average increases but then begins to level off, reaching approximately 3-4 Hz after 300 measurements. In general, this type of averaging can take a significant amount of time (during which time evaporation of the ink may occur) and still may not yield the desired resolution.

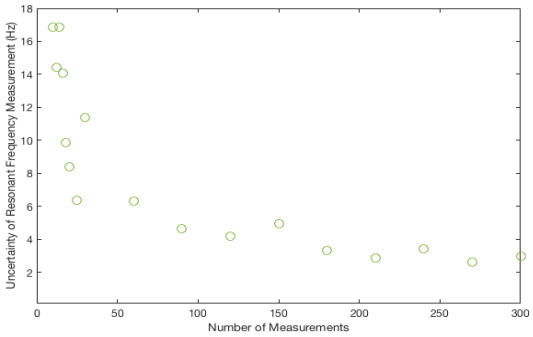

Fig. 6: Uncertainty of the average first peak frequency as determined by a Lorentzian fit to a thermal tune on an Asylum Research MFP-3D. Even averaging 200 measurements only yields an accuracy of 3-4 Hz.

IV. Stepped-Sine Measurement

The stepped-sine method to system identification drives the system using a sinusoid at a single frequency, integrating the response over an integer number of oscillations and calculating the in-phase and quadrature signals to extract the frequency response function (FRF) at the drive frequency. An entire FRF is measured by stepping (or sweeping) the drive frequency [20]. We give a brief description of the approach here to establish the elements needed for our algorithm. A complete description of the stepped-sine method can be found in [18], [20], [21].

For a linear time-invariant system, the steady state output to a driving sinusoid can be written as

$$s(t) = C\sin(\omega_0 t + \phi) + n(t), \tag{3}$$

where ω_0 is the drive frequency, C, ϕ and $n(t)$ are the output magnitude, phase, and measurement noise, respectively.

Our main interest here is to extract the magnitude of the signal. To achieve this, the output is first mixed with the in-phase and quadrature signals,

$$I(t) = s(t)\sin(\omega_0 t), \tag{4a}$$

$$Q(t) = s(t)\cos(\omega_0 t). \tag{4b}$$

To improve the SNR, the signals $I(t)$ and $Q(t)$ are averaged over an integer number M of periods of the drive signal to product the in-phase and quadrature sums,

$$I_{sum} \approx \frac{1}{MT_0}\int_0^{MT_0} I(t)dt, \tag{5a}$$

$$Q_{sum} \approx \frac{1}{MT_0}\int_0^{MT_0} Q(t)dt. \tag{5b}$$

Finally, the magnitude of the response at the drive frequency is easily calculated from the sum signals using

$$C = 2\sqrt{I_{sum}^2 + Q_{sum}^2}. \tag{6}$$

V. Overall Algorithm

In the DPN application, it is natural to do an accurate system identification before the writing process begins to identify the location of the original resonance frequency. Because the shift of the resonance after each write is small, this prior knowledge indicates the approximate location of the new peak and allows us to focus the measurements in a narrow band of frequencies. The essential idea of our algorithm, then, is to inject three different sinusoids spanning that frequency band, use the stepped-sine algorithm to extract the three magnitude values of the FRF, fit a model to these data using a nonlinear least squares fit, and extract the peak value. This estimate is then refined iteratively by selecting three new frequencies in a band with a narrower width centered on the new estimate, and terminating when the change in the frequency estimate between successive iterations is below a pre-defined threshold.

In AFM, the cantilever is typically driven using a piezo-actuator, either the same one used to control the z–position or one dedicated to the task. Under the assumption that each of these is well described by a second-order system, the joint transfer function is given by

$$G(s) = \left(\frac{a}{s^2 + bs + c}\right)\left(\frac{d}{s^2 + es + f}\right), \qquad (7)$$

where a, $b = 2\zeta_1\omega_1$ and $c = \omega_1^2$ are given by the gain, damping, and resonance frequency of the piezo, and d, $e = 2\zeta_2\omega_2$, and $f = \omega_2^2$ are given by the gain, damping and resonance frequency of the (primary mode) of the cantilever.

Using (7) to calculate the magnitude of the transfer function at a specific frequency ω_0 yields

$$\hat{C}(\omega_0) = \frac{a^2 d^2}{\sqrt{\omega_0^4 + ((-f - be - c)\omega_0^2 + cf)^2 + ((-e - b)\omega_0^3 + (bf + ce)\omega_0)^2}}. \qquad (8)$$

The DPN process changes only the mass on the cantilever. This primarily changes the resonance frequency of the cantilever but may also cause changes in its damping parameter. Under the reasonable assumption that the piezo dynamics are unmodified, the optimization problem to be solved is

$$\min_{\omega_2, \zeta_2} \frac{1}{n} \sum_{i=1}^{n} \left[C(\omega_0^i) - \hat{C}(\omega_0^i)\right]^2, \qquad (9)$$

where $C(\omega_0^i)$ $i = 1, ..., n$ are the measured magnitudes from (6). This nonlinear least squares problem can be solved numerically using an initial guess given by the previous values (with the first guess given by the previously identified modeled before the writing process was begun) and bounds on the optimization parameters chosen by the maximum amount of mass that can be deposited on the substrate during a write.

VI. Simulations

In this section we present simulation results to demonstrate our algorithm and to compare its performance to the standard measurement using a thermal. A piezo-actuator for the vertical displacement is in the range of 400 Hz and 3 kHz [22]. We use a true system with model given by (7). The piezo parameters were selected to be $\zeta_1 = 0.1$, $\omega_1 = 1$ kHz, and $a = \omega_1^2$ while the cantilever parameters were set to $\zeta_2 = 0.01$, $\omega_2 = 14$ kHz, and $d = \omega_2^2$ (motivated by theexperimental results in Sec. III). (Note that since thermal excitation only drives the cantilever dynamics, the experimental thermal results in Fig. 4 only show cantilever resonances.)

A. Thermal Measurement

To simulate a thermal, the cantilever system was driven with a zero mean Gaussian white noise process with a variance selected to approximately match the experimental results in Fig. 5. Data was acquired at a 4 MHz sampling rate for a total of approximately 33 milliseconds and then processed using an FFT. This was repeated 300 times (for a total of approximately 10 seconds of data) and the results averaged to improve the SNR before fitting a Lorentzian to the averaged results. This sequence was performed ten times to produce statistics on the estimate of the resonance frequency. The results of a typical run are shown in Fig. 7 with the simulated data in green and the Lorentzian fit in red.

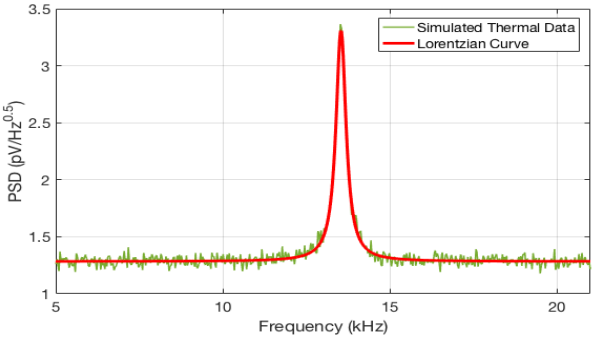

Fig. 7: A Lorentzian fit to the FFT of a simulated thermal measurement with white noise input and a 2% measurement noise in amplitude to the stepped sine algorithm. The frequency and damping of the cantilever are assumed to be 14 kHz and 0.01.

As shown in Fig. 8, the estimates values had errors ranging from -8 Hz to 6 Hz. Over the ten runs, the thermal method yielded an estimate of 13.998 kHz $\pm$ 2.482 Hz.

B. Stepped-Sine Method

The input signal to the stepped-sine method was simulated as a sinusoid with additive noise at a level of 2% of the signal amplitude. A typical signal is shown in Fig. 9. The output at each input frequency was sampled at 100 times of the selected frequency for 30 cycles. The sampling rate was set to get 100 samples per cycle.

A typical fitting result is shown in Fig. 10 with the fitted curve shown in green and the measured amplitudes shown in red. In the first iteration, measurements were made equi-spaced in a 100 Hz band. After estimating the resonance frequency, three new frequencies were selected, equi-spaced in band centered on that estimate but with a width that was

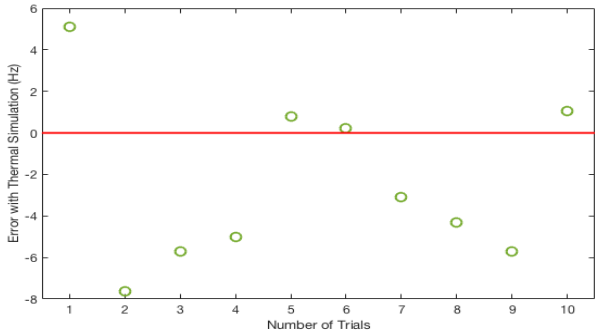

Fig. 8: Error in the thermal estimates in each simulation. The error ranged from -8 Hz to 6 Hz with an overall estimate of 13.998 kHz $\pm$ 2.482 Hz.

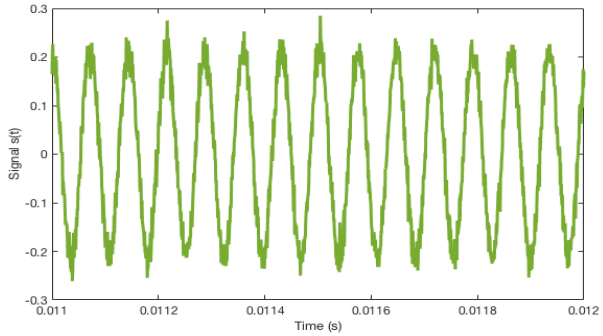

Fig. 9: Simulated input signal at 13.9 kHz with 2% measurement noise in amplitude added.

90% the width of the band at the previous step. This was iterated, halving the frequency band, until the change in the resonance frequency estimated from one iteration to the next was less than 0.1 Hz.

To compare the algorithm with the thermal method, 10 simulations were performed. The resulting estimation errors, shown in Fig. 11, ranged from -0.5 to 0.5 Hz. Over ten runs, the stepped-sine algorithm yielded 14.00 kHz $\pm$ 0.178 Hz.

Clearly, the stepped-sine algorithm outperformed the thermal technique in terms of resolution, easily meeting the requirement of 1 Hz. In addition, the method is quick since only a few cycles of a small number of high frequencies are needed. With the traditional thermal technique, the entire process can take nearly 20 seconds with 300 measurements. The stepped-sine technique, implemented in MATLAB, ran in approximately 0.7 seconds from beginning to end.

C. *Effect of parameter choices*

The performance of the stepped-sine algorithm depends on several parameter choices, most notably the number of cycles (M) to use when averaging the in-phase and quadrature sums, the number of frequency points to measure and use in the fit, and the termination condition.

To study the effect of M, simulations were performed varying the number of cycles from 1 to 140 with a fixed noise level at 2% of the signal amplitude. The results are shown in Fig. 12, indicating that, as expected, the performance

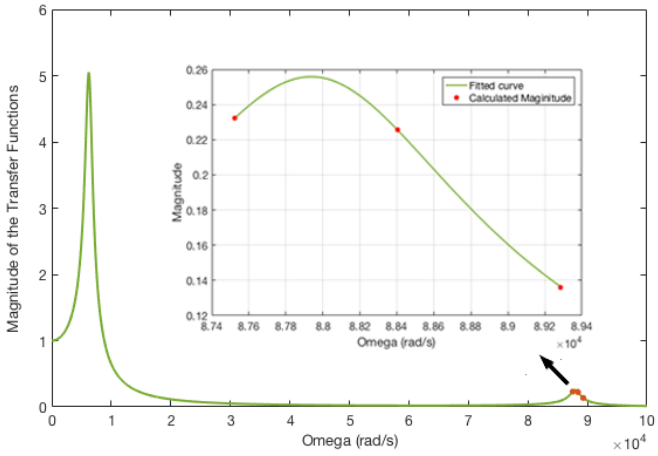

Fig. 10: Typical fitting result in the stepped-sine method. The first peak is the resonance of the piezo-actuator; the second peak is the cantilever. Red dots: measured magnitude values using the stepped-sine technique. Green curve: fit of the model to those measurements.

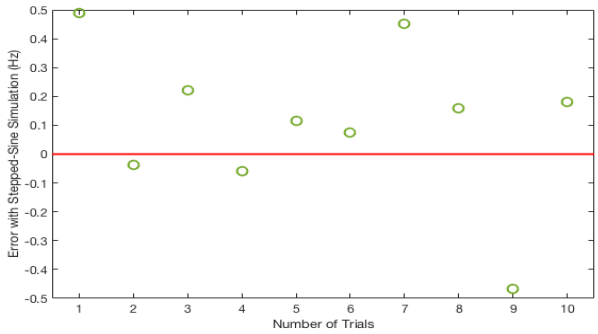

Fig. 11: Error in the stepped-sine based estimates in each simulation using averaging over 30 oscillations and terminating with a change in estimated frequency smaller than 0.1 Hz. The error ranged from -0.5 Hz to 0.5 Hz with an overall estimate of 14.00 Hz $\pm$ 0.178 Hz.

improvement slows as the number of oscillations increases. One should choose the smallest M that meets the resolution needed to optimize the overall time.

When considering the number of points to measure, one again would like to use as few as possible to keep the overall computation time low. To study this effect, simulations were performed with M=30 and a termination condition of 0.1 Hz but varying the number of points used. The resulting standard deviations in the estimate (over 10 simulation runs) are shown in Fig. 13. The simulations indicate that there is significant improvement in going from two to three points but that the resolution does not improve with higher numbers. This makes sense given that there are only two fitting parameters.

Finally, the choice of termination condition can affect the performance. At each step, the three measurement points get more closely spaced. Looking at Fig. 10, it is intuitively clear that if they get too close, noise will dominate and the three

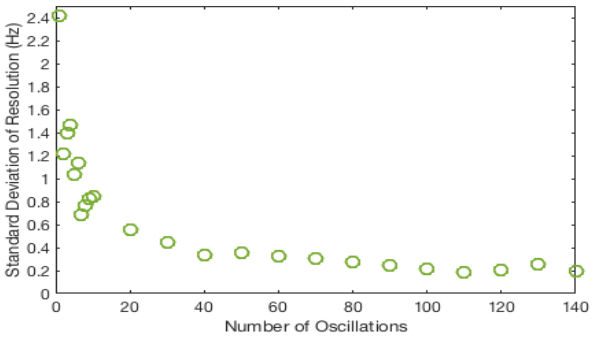

Fig. 12: Uncertainty in resonance frequency estimate as a function of M, the number of oscillations used to average the quadrature and in-phase signals. Simulations were performed with a noise level of 2%.

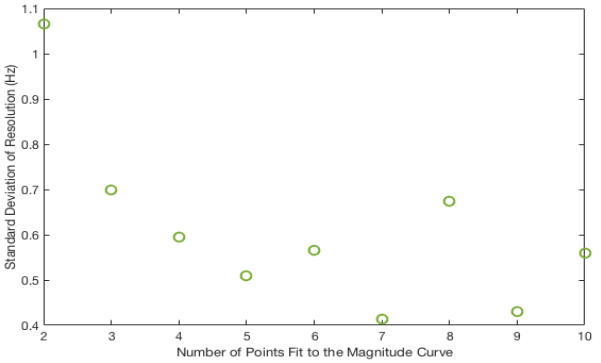

Fig. 13: Uncertainty in resonance frequency as a function of the number of points used for each fit. While there is improvement in going from two to three measurements, increasing the number of points further does not yield gains in accuracy.

measurements will not yield distinct information, leading to a poor estimate. If they are too far apart, they will be far from resonance and again the noise may dominate. In our iterative scheme, this implies the method should be terminated once a threshold, defined by the noise level (and, practically, the experience of the user) is met.

VII. Conclusions

This paper presented a stepped-sine curve-fit optimization method to measure quickly and accurately the shift of the resonance frequency of a scanning probe in an AFM during DPN. The combination of stepped-sine system identification, curve-fitting and iterative search optimization yields a scheme that takes advantage of the high signal-to-noise ratio offered by stepped-sine while remaining fast due to the small number of measurements needed. Simulation results indicate that the technique outperforms the standard thermal tune and yields a resolution better than needed for the DPN application.

Acknowledgements

This work supported in part by the NSF through CMMI-1661412.

References

[1] D. J. Muller, "AFM: A Nanotool in Membrane Biology," *Biochemistry*, vol. 47, no. 31, pp. 7986–7998, Aug. 2008.

[2] S. Liu and Y. Wang, "Application of AFM in microbiology: a review," *Scanning*, vol. 32, no. 2, pp. 61–73, Mar. 2010.

[3] W. Melitz, J. Shen, A. C. Kummel, and S. Lee, "Kelvin probe force microscopy and its application," *Surface Science Reports*, vol. 66, no. 1, pp. 1–27, Jan. 2011.

[4] K. Haase and A. E. Pelling, "Investigating cell mechanics with atomic force microscopy," *Journal of The Royal Society Interface*, vol. 12, no. 104, pp. 20 140 970–20 140 970, Mar. 2015.

[5] T. Ando, T. Uchihashi, and S. Scheuring, "Filming Biomolecular Processes by High-Speed Atomic Force Microscopy," *Chemical Reviews*, vol. 114, no. 6, pp. 3120–3188, Jan. 2014.

[6] Y. Ruan, A. Miyagi, X. Wang, M. Chami, O. Boudker, and S. Scheuring, "Direct visualization of glutamate transporter elevator mechanism by high-speed AFM," *Proceedings of the National Academy of Sciences*, vol. 114, no. 7, pp. 1584–1588, Feb. 2017.

[7] C. Yang, R. Winkler, M. Dukic, J. Zhao, H. Plank, and G. E. Fantner, "Probing the Morphology and Evolving Dynamics of 3D Printed Nanostructures Using High-Speed Atomic Force Microscopy," *ACS Applied Materials & Interfaces*, vol. 9, no. 29, pp. 24 456–24 461, Jul. 2017.

[8] D. Y. Abramovitch, S. B. Andersson, L. Y. Pao, and G. Schitter, "A Tutorial on the Mechanisms, Dynamics, and Control of Atomic Force Microscopes," in *Proc. American Control Conference*, 2007, pp. 3488–3502.

[9] J. L. Hutter and J. Bechhoefer, "Calibration of atomic-force microscope tips," *Review of Scientific Instruments*, vol. 64, no. 7, pp. 1868–1873, 1993.

[10] M. T. Arjmand, H. Sadeghian, H. Salarieh, and A. Alasty, "Chaos control in AFM systems using nonlinear delayed feedback via sliding mode control," *Nonlinear Analysis: Hybrid Systems*, vol. 2, no. 3, pp. 993–1001, 2008.

[11] B. Capella and G. Dietler, "Force-distance curves by atomic force microscopy," *Surface Science Reports*, vol. 34, no. 1-3, pp. 1–104, 1999.

[12] M. Radmacher, R. W. Tillmann, and H. E. Gaub, "Imaging viscoelasticity by force modulation with the atomic force microscope," *Biophysical Journal*, vol. 64, no. 3, pp. 735–742, 1993.

[13] M. Radmacher, M. Fritz, and P. K. Hansma, "Imaging soft samples with the atomic force microscope: gelatin in water and propanol," *Biophysical Journal*, vol. 69, no. 1, pp. 264–270, 1995.

[14] S. N. Magonov and D. H. Reneker, "Characterization of Polymer Surfaces With Atomic Force Microscopy," *Annual Review of Materials Science*, vol. 27, no. 1, pp. 175–222, 1997.

[15] D. S. Ginger, H. Zhang, and C. A. Mirkin, "The Evolution of Dip-Pen Nanolithography," *Angewandte Chemie - International Edition*, vol. 43, no. 1, pp. 30–45, 2004.

[16] A. Urtizberea and M. Hirtz, "A diffusive ink transport model for lipid dip-pen nanolithography," *Nanoscale*, vol. 7, no. 38, pp. 15 618–15 634, 2015.

[17] N. Farmakidis, "Towards a Closed-Loop Nanolithography: Quantifying Ink Dynamics in Dip-Pen Nanolithography," 2016.

[18] D. Y. Abramovitch, "Built-in stepped-sine measurements for digital control systems," in *Proc. IEEE Conference on Control and Applications*, 2015, pp. 145–150.

[19] E. O. Sunden, T. L. Wright, J. Lee, W. P. King, and S. Graham, "Room-temperature chemical vapor deposition and mass detection on a heated atomic force microscope cantilever," *Applied Physics Letters*, vol. 88, no. 3, pp. 1–3, 2006.

[20] D. Y. Abramovitch, "Low latency demodulation for Atomic Force Microscopes, Part I efficient real-time integration," in *Proc. American Control Conference*, 2011, pp. 2252–2257.

[21] ——, "Low Latency Demodulation for Atomic Force Microscopes, Part II: Efficient Calculation of Magnitude and Phase," in *Proc. IFAC World Congress*.

[22] O. E. Rifai and K. Youcef-Toumi, "Coupling in piezoelectric tube scanners used in scanning probe\nmicroscopes," *Proceedings of the 2001 American Control Conference. (Cat. No.01CH37148)*, vol. 4, pp. 3251–3255, 2001.